Proceedings of the 3rd International Conference on Mechanical Engineering and Mechatronics
Prague, Czech Republic, August 14-15, 2014
Paper No. 166

PZT-based Modal Sensing and Compensation for Vibration Control of Moving Flexible Links

Xuping Zhang
Aarhus University, School of Engineering & Department of Engineering
2 Dalgas Avenue, 8000 C Aarhus, Denmark
xuzh@iha.dk

J. K. Mills, W. L. Cleghorn
University of Toronto, Department of Mechanical Engineering
5 King's College Road, Toronto, Ontario, Canada M5S 3G8
mills@mie.utoronto.ca; cleghrn@mie.utoronto.ca

Abstract **-** Increasing attention and efforts have been made to the active vibration control space-based flexible structures using Lead Zirconate Titanate (PZT) transducers. This work extends the active vibration control method to vibration suppression of moving links mounted on multi-body mechanical systems. A compressive methodology to control the vibration of the intermediate links is presented with the consideration of vibration mode coupling, unmodelled modes, uncontrolled modes, closely spaced modes, etc. To design the vibration controller in the modal space and prevent spillover, the independent modal space control (IMSC) method is employed. The modal filtering and compensation are addressed with details to implement IMSC method. Experimental results of a multi-body mechanical system with flexible links are given to verify the presented vibration control methods.

Keywords**:** PZT, Modal space, Modal filters, Modal compensators, Flexible links, Vibration control.

1. Introduction

Actuators and sensors made from piezoelectric materials, such as PZT, have been gaining considerable acceptance as means for vibration control of flexible structures in recent decades, because of the advantageous properties of piezoelectric materials (Preumont, 2002). These properties include mechanical simplicity, small volume, light weight, large bandwidth, efficient conversion between electrical energy and mechanical energy, and simple integration with various metallic and composite structures.

Compared with significant efforts and progress made to the simulation and experiment demonstrations of active vibration control in the space-based flexible structures and simple flexible beams using PZT sensors and actuators (Bailey and Hubbard, 1985), a few researchers have tried to extend such active vibration control methods to multi-body mechanical systems having flexible components (Liao and Sung, 1993). It is very different from flexible structures and simple beams in that rigid body motion and elastic deformation are dynamically coupled for flexible links in the multi-body mechanical systems (robot manipulators or mechanisms). This characteristic leads to the coupling of vibration modes, and may cause spillover. Moreover, the dynamic responses measured by PZT sensors include the unmodeled or unknown dynamics, including for example, compliance and clearance dynamics from the bearings, ball screw mechanisms, and motors. Therefore, the vibrations of the intermediate links are very complicated, and are the combination of free structural vibrations and forced vibrations, which contain many frequency components which are closely spaced.

Spillover might also come from the uncontrolled modes as a limited small number of modes of flexible links can be or are required to be controlled in practice. The spillover causes control energy flows to the uncontrolled modes of the system, and results in instability and degradation of control performance (Preumont, 2002). Therefore, the independent modal space control (IMSC) method (Meirovitch and Baruh, 1981, Baz and Poh, 1988, Singh et al., 2003, Baz et al., 1992) must be employed to prevent from the spillover problem by controlling each mode separately. In the IMSC, the modal coordinates and/or modal velocities for the modes targeted for control must be real-time measured and monitored. There are three methods that can be used to extract the modal coordinates from the outputs of the sensors. These methods include state observers (Brogan, 1974), temporal filters (Hallauer et al., 1982), and modal filters (Meirovitch and Baruh, 1985). It has been shown that the use of observers causes observation spillover from the residual modes, which can destabilize the residual modes. Using temporal filters, the outputs of sensors are processed using high-pass or low-pass filters to filter out the contribution of each mode. Such a method does not work for the cases where the modes are closely spaced. Using modal filters, the task of extracting modal coordinates from the sensor outputs is distinct from the control task, which permits the use of modal filters in conjunction with any modal feedback control method. Furthermore, modal filters only involve spatial integration, which is a smoothing operation that can not lead to instability. Two different modal filtering methods have been presented for modal filters. One is a modal filter with a distributed element (Collins et al., 1994). The other is a modal filter with discrete elements (Sumali et al., 2001). It is often difficult to implement modal filtering with a distributed element because it requires one sensor for each mode. Therefore, it is reasonable to perform modal filtering with discrete sensors in real time. Sensing modal coordinates in real time involves interpolations or curve fitting. All computations must be carried out within a single sampling period because the controllers are implemented in discrete time.

Several feedback control techniques have been developed for vibration control, including angular velocity feedback (Bailey and Hubbard, 1985), L-type linear velocity feedback (Sun et al., 2004), strain feedback and strain rate feedback (Song et al. 2000), of the controlled points on flexible structures. Strain rate feedback (SRF) has a wider active damping frequency range, and hence can stabilize more than one mode simultaneously, given sufficient bandwidth (Song et al. 2000). To design and implement a SRF controller in the modal space, the simplified modal filters are used to measure the modal coordinates and velocities. To prevent probable destabilization resulted from the differentiation of the SRF controller, a compensator is needed to cut off the amplified noises and unmodeled dynamic signals with high frequencies, especially for the intermediate links in multi-body mechanical systems.

This work presents a comprehensive active vibration control methodology of moving flexible links in multi-body mechanical systems using PZT transducers. The vibration characteristics of moving flexible links are analyzed with the consideration of coupling dynamics and unmodeled dynamics in section II. The SRF controller design in modal space is presented in Section III. The design modal filters and compensators are addressed with details respectively in Section IV and V. In Section IV, the experimental results are given to validate the presented active vibration control strategies and methods. Combined with the presented methodology and strategy in this work, the discussions and conclusions are made in the last section to provide compressive insight and guidance for actively controlling the vibration of moving flexible links in multi-body mechanical systems using PZT transducers.

2. Modal Dynamics of Moving Active-Structures

An active vibration control structure is designed and built by bonding PZT sensors/actuators to the two sides of a flexible link as shown in Figure 1. The PZT patches on one side of the link act as sensors, while the PZT patches on the opposite link face act as actuators. One sensor and one actuator constitute a PZT control pair based on the strain rate feedback control strategy, and are located at the same location along the length of each intermediate link.

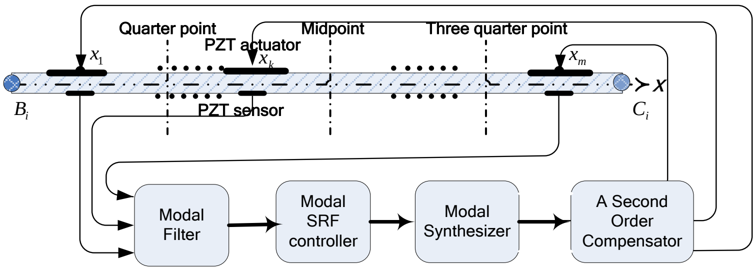

Fig. 1. A smart link structure with PZT actuator and sensor patches (Zhang et al., 2009).

Using the assumed mode method based on the boundary conditions, the dynamic equation of a moving link can be given in modal space as

$$\ddot{\bar{\boldsymbol{\eta}}} + C\dot{\bar{\boldsymbol{\eta}}} + \boldsymbol{\Omega}\bar{\boldsymbol{\eta}} = \bar{F}_{\mathbf{w}} + \bar{F}_{\mathbf{u}} \tag{1}$$

where $\bar{\boldsymbol{\eta}} = [\eta_1 \quad \cdots \quad \eta_n]^T$ is the modal coordinate vector of an intermediate link, $C = diag(2\xi_i m_{ii}\omega_i)$ is the modal damping matrix based on the assumption of Rayleigh damping, $\boldsymbol{\Omega} = diag(\omega_i^2)$ is the structural modal stiffness matrix, ω_i is the i^{th} order modal frequency, and $\bar{F}_{\mathbf{w}}$ reflects the modal force from the effect of the rigid-body motion on the elastic vibration of the flexible links, the coupling between the rigid-body motions and the elastic motions, and other unmodelled forces. $\bar{F}_u$ is the modal control force vector transformed from bending moment created by PZT actuators.

3. Modal Strain Rate Feedback Controller

One active vibration control strategy is direct output feedback control (DOFC) (strain or/and strain rate). This control approach does not demand modal state estimation. In this method, the sensors are collocated with the actuators, and a given actuator control force is a function of the sensor output at the same location along the intermediate link. Thus, one PZT actuator and one PZT sensor constitute a PZT control pair based on the strain and strain rate feedback control strategy. Using strain and strain rate feedback, the control voltage applied a PZT actuator (center point of the PZT actuator) located at along the intermediate link is given as,

$$\begin{aligned} V_a(t) &= -k_p V_s(t) - k_d \dot{V}_s(t) \\ &= -K_s \left\{ k_p \sum_{i=1}^{n} \left[\varphi_i^{''}(x_k)\eta_i(t) \right] + k_d \sum_{i=1}^{n} \left[\varphi_i^{''}(x_k)\dot{\eta}_i(t) \right] \right\} \end{aligned} \tag{2}$$

where k_p and k_d are the feedback gains in terms of voltages and voltage rates, V_s the voltage picked up the corresponding PZT sensor, and φ_i the i^{th} modal shape function of the link. The modal force vector produced by the PZT actuator is expressed as

$$\bar{\mathbf{F}}_u = -K_s K_a \begin{bmatrix} (\varphi_1^{'}(x_k^2) - \varphi_1^{'}(x_k^1))\varphi_1^{''}(x_k) & \cdots & (\varphi_1^{'}(x_k^2) - \varphi_1^{'}(x_k^1))\varphi_n^{''}(x_k) \\ \vdots & \vdots & \vdots \\ (\varphi_n^{'}(x_k^2) - \varphi_n^{'}(x_k^1))\varphi_1^{''}(x_k) & \cdots & ((\varphi_n^{'}(x_k^2) - \varphi_n^{'}(x_k^1)))\varphi_n^{''}(x_k) \end{bmatrix} \bullet \left[k_p \begin{pmatrix} \eta_1 \\ \vdots \\ \eta_n \end{pmatrix} + k_d \begin{pmatrix} \dot{\eta}_1 \\ \vdots \\ \dot{\eta}_n \end{pmatrix} \right] \tag{3}$$

where x_k^2 is the coordinate at the right end of the PZT actuator, and x_k^1 is the coordinate at the left end of the PZT actuator. Note that we assume that all PZT sensors are identical, and all PZT actuators are identical in this work. In practice, the controller is designed with only the limited low order mode targeted for control (for example, c modes). Equation (3) can be partitioned and written as

$$\bar{\mathbf{F}}_u = \begin{bmatrix} \bar{\mathbf{F}}_{\mathbf{c}} \\ \bar{\mathbf{F}}_{\mathbf{n-c}} \end{bmatrix} = \begin{bmatrix} \boldsymbol{\psi}_{\mathbf{c,c}} & \boldsymbol{\psi}_{\mathbf{c,n-c}} \\ \boldsymbol{\psi}_{\mathbf{n-r,c}} & \boldsymbol{\psi}_{\mathbf{n-c,,n-c}} \end{bmatrix} \left[k_p \begin{pmatrix} \eta_1 \\ \vdots \\ \eta_c \\ \eta_{c+1} \\ \vdots \\ \eta_n \end{pmatrix} + k_d \begin{pmatrix} \dot{\eta}_1 \\ \vdots \\ \dot{\eta}_c \\ \dot{\eta}_{c+1} \\ \vdots \\ \dot{\eta}_n \end{pmatrix} \right] = \begin{bmatrix} \boldsymbol{\psi}_{\mathbf{c,c}}(\mathbf{k_p}\bar{\boldsymbol{\eta}}_{\mathbf{c}} + \mathbf{k_d}\dot{\bar{\boldsymbol{\eta}}}_{\mathbf{c}}) + \boldsymbol{\psi}_{\mathbf{c,n-c}}(\mathbf{k_p}\bar{\boldsymbol{\eta}}_{\mathbf{n-c}} + \mathbf{k_d}\dot{\bar{\boldsymbol{\eta}}}_{\mathbf{n-c}}) \\ \boldsymbol{\psi}_{\mathbf{n-c,c}}(\mathbf{k_p}\bar{\boldsymbol{\eta}}_{\mathbf{c}} + \mathbf{k_d}\dot{\bar{\boldsymbol{\eta}}}_{\mathbf{c}}) + \boldsymbol{\psi}_{\mathbf{n-c,n-c}}(\mathbf{k_p}\bar{\boldsymbol{\eta}}_{\mathbf{n-c}} + \mathbf{k_d}\dot{\bar{\boldsymbol{\eta}}}_{\mathbf{n-c}}) \end{bmatrix} \tag{4}$$

In equation (4), $\bar{F}_c$ is the modal control force for the targeted modes. $\bar{\mathbf{F}}_{\mathbf{n-c}}$ is the modal control force flow into the uncontrolled modes, and it could result the control spillover. The term $\boldsymbol{\psi}_{\mathbf{c,n-c}}(\mathbf{k_p}\bar{\boldsymbol{\eta}}_{\mathbf{n-c}} + \mathbf{k_d}\dot{\bar{\boldsymbol{\eta}}}_{\mathbf{n-c}})$ in $\bar{F}_c$ is caused by the excited uncontrolled modes flowing to the modes targeted for control. The interactive action between controlled modes and uncontrolled modes finally could lead to the instability of the control system. Furthermore, it is clear that the control force is coupled among the controlled modes since the matrix $\begin{bmatrix} \mathbf{\Psi}_{\mathbf{c,c}} & \mathbf{\Psi}_{\mathbf{c,n-c}} \\ \mathbf{\Psi}_{\mathbf{n-r,c}} & \mathbf{\Psi}_{\mathbf{n-c,,n-c}} \end{bmatrix}$ in equation (4) is not a diagonal matrix, and hence the controlled modes are dependent of each other. As a result, it is difficulty, if not impossible to determine control gains to suppress the vibration when multiple PZT actuators are applied. The reason for that is that pole allocation or optimal control most likely will require gain matrices with entries independent of each other while DOFC implies that the entries of the control gain matrix are not independent for multi-actuators.

To prevent control spillover, a phenomenon that results in degradation of performance or instability, the Independent Modal Space Control (IMSC) is employed for the controller design in this work. Using modal coordinates, a feedback control problem of continuous structures can be transformed to the problem of controlling several single-degree-of-freedom (SDOF) systems in parallel, with no interaction among the systems. Therefore, feedback controllers can be designed in the independent modal space so that each targeted mode is controlled by one independent modal controller associated with only its own modal displacement and velocity. With IMSC, the modal control force f_u^i for the i^{th} mode only depends on η_i and $\dot{\eta}_i$. f_u^i is given as

$$f_u^i = -k_p^i \eta_i - k_d^i \dot{\eta}_i \tag{5}$$

Equation (5) illustrates that the coupling of modal equations due to feedback is avoided with IMSC. Combining equations (1) and (3), the closed-loop modal equations can be expressed with the independent modes as

$$\ddot{\eta}_i + (2\xi_i \omega_i + k_d^i)\dot{\eta}_i + (\omega_i^2 + k_p^i)\eta_i = f_w \qquad i = 1, \cdots, \quad n \tag{6}$$

Many approaches, such as pole assignment or optimal control, exist to determine the control gain in Equation (6). In the optimal control approach the control gains are determined through optimizing a prescribed performance index. In the IMSC method, a quadratic function, the combination of the modal potential energy $\omega_i^2 \eta_i^2$, modal kinetic energy $\dot{\eta}_i^2$, and the required modal control force f_u^i, is typically chosen to be the performance index given as

$$J = \int_0^\infty \left[(\omega_i^2 \eta_i^2 + \dot{\eta}_i^2) + \beta (f_u^i)^2 \right] dt \tag{7}$$

In Equation (7), β is modal weight used to signify the importance of vibration energy suppression and the required control effort. The closed-loop solution to Equation (7) can be obtained by solving a matrix Riccati equation, and is given as

$$\begin{cases} k_p^i = -\omega_i^2 + \omega_i (\omega_i^2 + \beta^{-1})^{1/2} \\ k_d^i = -2\xi_i \omega_i + [4\xi_i^2 \omega_i^2 + \beta^{-1} - 2\omega_i^2 + 2\omega_i (\omega_i^2 + \beta^{-1})^{1/2}]^{1/2} \end{cases} \tag{8}$$

4. Modal Filter and Synthesizer

In practical experiments, the output voltage of a PZT sensor corresponds to the physical link physical deformation coordinates, not modal coordinates. Therefore, to implement IMSC control, the modal coordinates must be extracted from the output voltages of discrete PZT sensors in real time. The modal coordinates, extracted in real time, are provided to the modal feedback controller. Using the modal synthesizer, the modal control voltages are transformed back to the control voltages in physical space, and are used as inputs to the PZT actuators.

The implementation of IMSC is illustrated in Figures 1 and 2. Note that we assume all PZT sensors are identical, and PZT actuators are identical as well. Since the length of PZT actuators is much smaller than the length of intermediate links, $\varphi_i^{'}(x_k^R)-\varphi_i^{'}(x_k^l)$ is approximated to be $\varphi_i^{''}(x_k)l_a$, where l_a is the length of a PZT actuator.

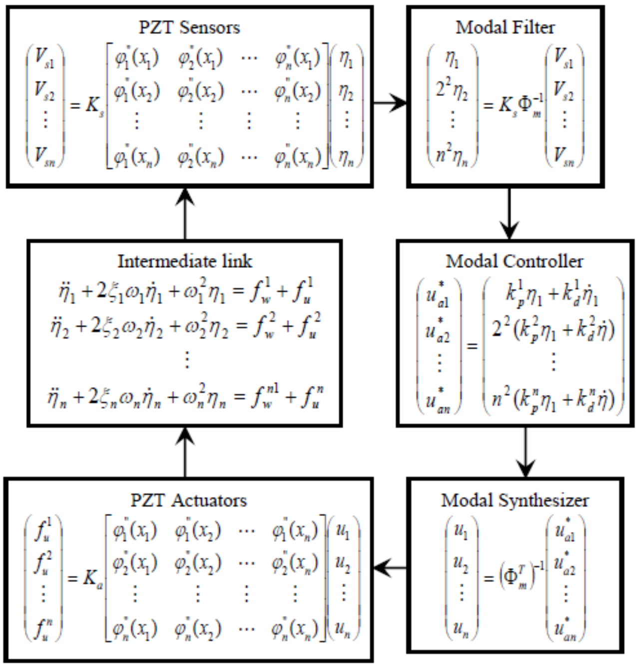

Fig. 2. Schematic of IMSC implementation based on PZT transducers (Zhang et al., 2009).

The modal filter expression for each smart link is expressed as

$$\bar{\boldsymbol{\eta}}(\mathbf{t})=\boldsymbol{\Phi}_{\mathbf{m}}\bar{\mathbf{V}}_{\mathbf{s}}(\mathbf{t}) \tag{9}$$

where $\bar{\boldsymbol{\eta}}_i=(\eta_1(t) \quad \eta_2(t) \quad \cdots \quad \eta_n(t))^T$ is modal coordinate vector of the intermediate link, $\bar{\mathbf{V}}_{\mathbf{s}}=(V_{s1}(t) \quad V_{s2}(t) \quad \cdots \quad V_{sm}(t))^T$ is the output vector of the m sensors bonded to the intermediate link, and $\boldsymbol{\Phi}_{\mathbf{m}}$ is a $n \times m$ modal coordinate transformation matrix or modal analyzer. $\boldsymbol{\Phi}_{\mathbf{m}}$ is given as

$$\boldsymbol{\Phi}_{\mathbf{m}}=\frac{\mathbf{1}}{\mathbf{K}_{\mathbf{s}}}(\boldsymbol{\psi}^T\boldsymbol{\psi})^{-1}\boldsymbol{\psi}^T \tag{10}$$

The matrix $\boldsymbol{\psi}$ is calculated with the values of the mode shape function at the discrete sensors

$$\boldsymbol{\psi}=\begin{bmatrix} \varphi_1(x_1) & \varphi_2(x_1) & \cdots & \varphi_n(x_1) \\ \varphi_1(x_2) & \varphi_2(x_2) & \cdots & \varphi_n(x_2) \\ \vdots & \vdots & \cdots & \vdots \\ \varphi_1(x_m) & \varphi_2(x_m) & \cdots & \varphi_n(x_m) \end{bmatrix} \tag{11}$$

As shown in Figures 1 and 2, the modal coordinates, extracted in real time, are provided to the modal feedback controller. Using the modal synthesizer, the modal control voltages are transformed to the control voltages in physical space, and are used as inputs to the PZT actuators.

5. Modal Compensator Design

The implementation of the derivative algorithm tends to amplify noise or the unmodeled vibration signal at higher frequencies due to its derivative operation. In practice, it is desirable to add a compensator so that the SRF controller exhibits guaranteed stability and a larger roll-off at high frequency (Song et al. 2000). The basic idea is to pass the strain rate feedback signal through a second order filter with substantial damping, and generate a feedback proportional to the output of the filter. To better illustrate the operation principle of SRF controller with a compensator, it is assumed that a structure may be simplified to be a single degree of freedom, single-input-single-output vibration system using one collocated PZT sensor and actuator pair. The block diagram which describes the control strategy is shown in Figure 3.

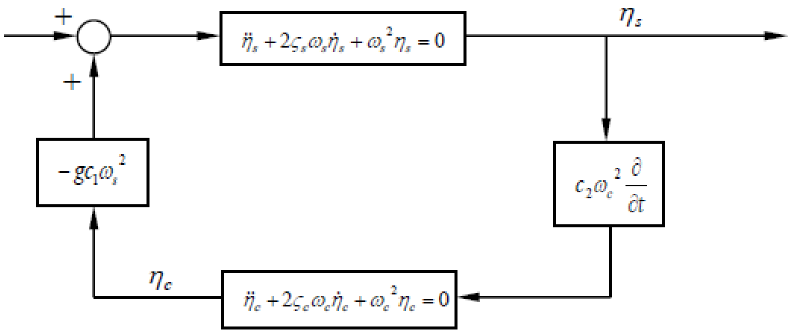

Fig. 3. Block diagram for SRF controller with compensator (Zhang et al., 2009).

The equations of the system and the compensator for SRF control are expressed as in (Song et al. 2000)

$$\ddot{\eta}_s + 2\varsigma_s\omega_s\dot{\eta}_s + \omega_s^2\eta_s = -gc_1\omega_s^2\eta_c \tag{13}$$

$$\ddot{\eta}_c + 2\varsigma_c\omega_c\dot{\eta}_c + \omega_c^2\eta_c = c_2\omega_c^2\dot{\eta}_s \tag{14}$$

where η_s is a modal coordinate of the structure, ς_s is the damping ratio of the structure, ω_s is the natural frequency of the structure, η_c is a modal coordinate of the compensator, ς_c is the damping ratio of the compensator, ω_c is the resonant frequency of the compensator, g is a strain rate back feedback gain, c_1 and c_2, are constants which are determined by the sensitivity of the actuator and sensor, respectively. It should be noted that equation (13) and equation (14) are coupled by the physical interaction between control signals, through the coordinate η_s, and the structure.

Assume that the vibration solution for the structure with a single degree of freedom is given in the form as

$$\eta_s = \mu e^{i\omega_s t} \tag{15}$$

The steady vibration solution of the compensator is given as

$$\eta_c = \lambda e^{i(\omega_s t + \pi/2 - \phi)} \tag{16}$$

where $\lambda = c_2\mu\omega_s\omega_c / \sqrt{(1-\omega_s^2/\omega_c^2)^2 + (2\varsigma_c\omega_s/\omega_c)^2}$ and $\phi = \tan^{-1}\left[(2\varsigma_c\omega_s/\omega_c)/(1-\omega_s^2/\omega_c^2)\right]$.

From equation (15) and equation (16), we have

$$\eta_c = \lambda e^{i(\omega_s t)} e^{i(\pi/2-\phi)} = \frac{c_2\omega_s\omega_c e^{i(\frac{\pi}{2}-\phi)}}{\sqrt{(1-\omega_s^2/\omega_c^2)^2 + (2\varsigma_c\omega_s/\omega_c)^2}}\eta_s \tag{17}$$

Substituting equation (17) into equation (13), the structural vibration equation with SRF controller is expressed as three different forms with the relationship between the structural natural frequency, ω_s, and the compensator resonant frequency, ω_c. When $\omega_s << \omega_c$, the phase angle approaches ϕ zero. Substituting equation (17) into (13), equation (13) can be formulated as

$$\ddot{\eta}_s + (2\varsigma_s + gc_1\lambda)\omega_s\dot{\eta}_s + \omega_s{}^2\eta_s = 0 \tag{18}$$

Equation (18) clearly shows that the essential role of the SRF compensator is to increase the damping ratio of the structure. When $\omega_s = \omega_c$, the phase angle ϕ is equal to $\pi/2$. Substituting equation (17) into (13), equation (13) can be expressed as

$$\ddot{\eta}_s + 2\varsigma_{s1}\omega_s\dot{\eta}_s + (\omega_s{}^2 + gc_1\lambda\omega_s{}^2)\eta_s = 0 \tag{19}$$

Equation (19) shows that the SRF compensator leads to the increase of the stiffness of the structure. When $\omega_s >> \omega_c$, the phase angle ϕ approaches π. Substituting equation (17) into equation (13), equation (13) can be presented as

$$\ddot{\eta}_s + (2\varsigma_s - gc_1\lambda)\omega_s\dot{\eta}_s + \omega_s{}^2\eta_s = 0 \tag{20}$$

Equation (20) demonstrates that the compensator tends to decrease the damping ratio of the structure in this case. Therefore, in the design of SRF control with the compensator (filter), the compensator should be designed to make sure that the targeted frequencies are below the compensator frequencies. The above strategy can be extended to control multiple modes by introducing multiple compensators in parallel. One compensator is designed for each targeted mode.

6. Experimental Validation

In this work, three PZT sensors and actuators are bonded to the third intermediate link at its quarter point, midpoint and three-quarter point, as shown in Fig.4. Three actuators and sensors are selected as BM 532, manufactured by Sensor Technology. The piezoelectric constant d_{31} is $-270\times10^{-12}C/N$, and Young's modulus is $6.3\times10^{10}N/m^2$. The dimensions of each PZT actuator are $25.4mm\times25.4mm\times0.254mm$ and the dimensions of each PZT sensor are $6.35mm\times6.35mm\times0.254mm$. The active vibration control system is set up using LabVIEW Real-Time (Zhang et al., 2009). The sampling rate for each channel of the A/D and D/A is configured to be 1000 *Hz*, and the input and output voltage range of each channel of the A/D and D/A is set to be volts. The voltage gain for each channel of the Sensor Technology SS08 amplifier is set to be 30.

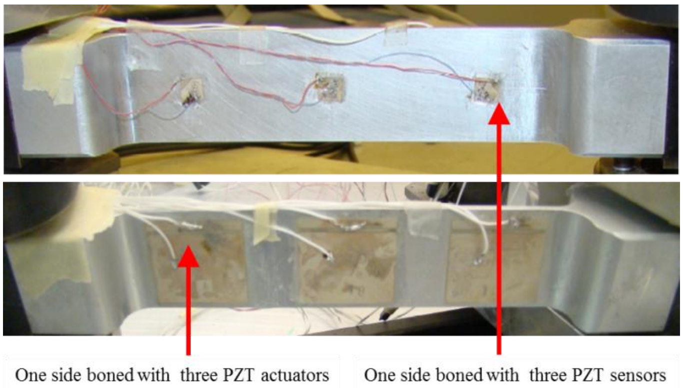

Fig. 4. Intermediate link bonded with PZT transducers (Zhang et al., 2009).

The three flexible links were mounted into a 3-PRR parallel robot manipulator whose end-effector moved around circular trajectory with a radius of 30mm, and modal testing are conducted using impact hammer and accelerometers (Zhang et al., 2007).To excite the structural vibration of the flexible intermediate links as much as possible, the maximum velocity and acceleration of three sliders were experimentally set to be 0.1 m/s and 50 m/s^2, respectively.

The theoretically designed gains may not be exactly optimal due to the uncertainty of the dynamic model and some other unconsidered factors, such as the phase transfer properties for low pass filters between D/As to the high-voltage PZT amplifiers. Therefore, using trial and error to adjust the gains, the poles of the flexible link were allocated to a desired location where best vibration attenuation results were achieved.

In this work, the first two flexible link modes are targeted for control. The control gains for the controlled modes are determined using the proposed strategy. Since the main purpose is to damp the vibration, only modal strain rate feedback is applied in the experiments. The control effort weighing is chosen as in Equation (7). Before the control suppression is implemented, the response of the uncontrolled system is analyzed using modal filters to obtain modal displacement and velocities. With the identified natural frequencies (the natural frequency is 75 Hz for the first mode, and 235 Hz for the second mode), the weight factor of the control gain of the second mode can be calculated using equation 8. The control gain for the first mode is selected to be 3.0, and the control gain for the second mode is selected to be 0.6. With these control gains, the first two modes are significantly suppressed for the all three flexible intermediate links bonded with PZT transducers. As shown in Figures 5-7, the vibration response measured at the quarter point, midpoint, and three-quarter point are significantly reduced. Figures 8 and 9 further show that the first mode vibration of the intermediate link was suppressed 70%, and Figures 10 and 11 demonstrate the second mode vibration is also decreased by 50%.

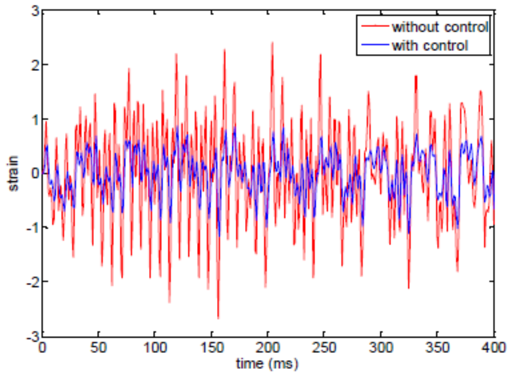

Fig. 5. Vibration at the quarter point.
(Zhang et al, 2009)

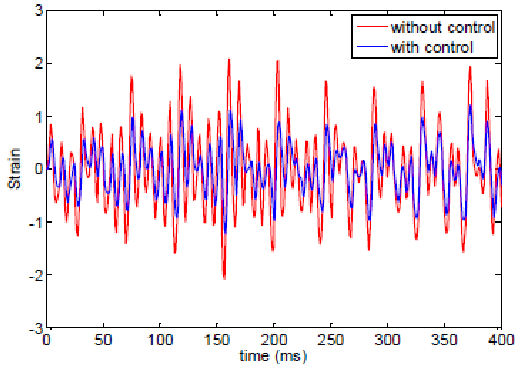

Fig. 6. Vibration at the midpoint.
(Zhang et al, 2009)

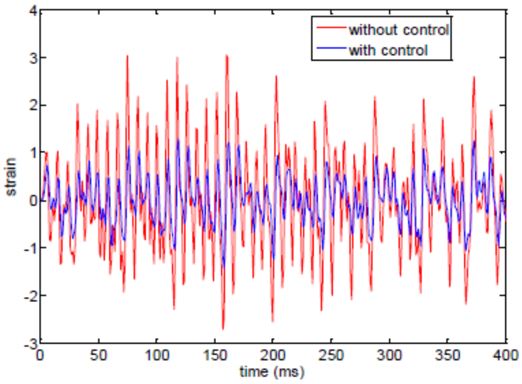

Fig. 7. Vibration at the three (Zhang et al, 2009).

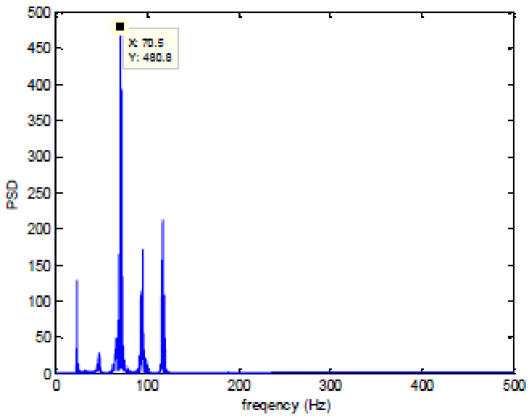

Fig. 8. FFT of mode 1 of link3 without control.

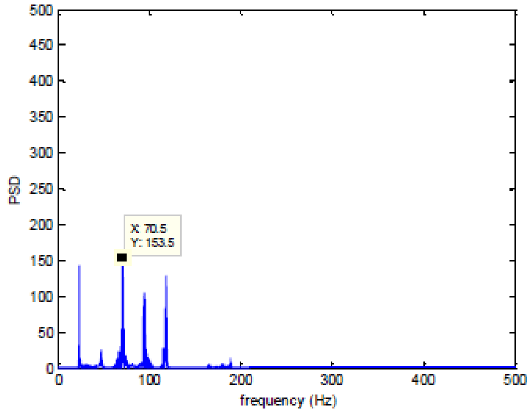

Fig. 9. FFT of model of Link3 with control

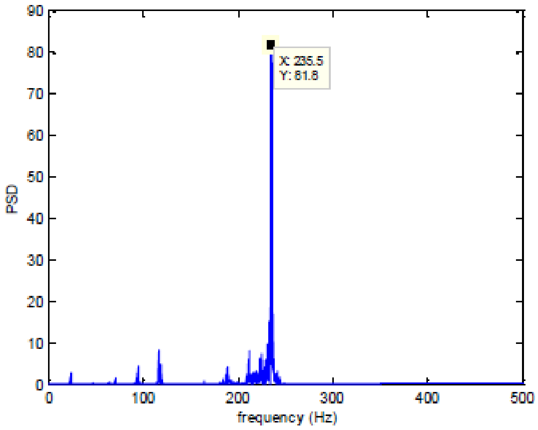

Fig. 10. FFT of mode 2 of Link3 without control.

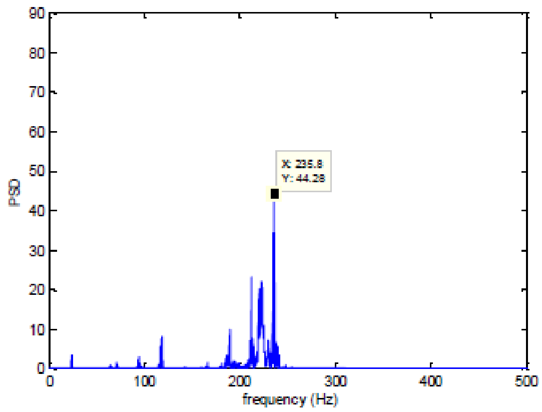

Fig. 11. FFT of mode 2 of link3 without control.

7. Discussion and Conclusion

A PZT-based active vibration control strategy is presented for moving flexible links mounted on multi-body mechanical systems using modal filters and second compensators based on the IMSC strategy. The modal filters are simplified and designed with assumed mode shapes. The proposed modal filters are used for the on-line estimation of modal coordinates and modal velocity. The second compensator is used to cut off the amplified noises and unmodeled dynamics due to the differentiation operation in the proposed controller. The modal coupling behavior of intermediate links is examined with the modal analysis of vibrations measured by the PZT sensors. An efficient multi-mode vibration control strategy has been proposed through modifying the IMSC strategy. Finally, active vibration control experiments are successfully implemented to three flexible links, each of which are equipped with three PZT control pairs at its quarter point, midpoint, and three quarter point. The experimental results show that the vibration of the flexible manipulator is suppressed effectively.

References

Bailey T., and Hubbard J. J. (1985). Distributed piezoelectric-polymer active vibration control of a cantilever beam. J. Guidance, Control and Dynamics, 9(5), 605–611.

Baz A., and Poh S. (1988). Performance of an active control system with piezoelectric actuators. Journal of Sound and Vibration, 126 (2), 327-343.

Baz A., Poh S., and Fedor J. (1992). Independent modal space control with positive position feedback. Journal of Dynamic systems, Measurement and Control, 114, 96-103.

Brogan W. L. (1974). “Modern Control Theory” Quantum Publishers, New York.

Collins S. A., Miller D. W., and Flotow A. H. (1994). Distributed sensors as spatial filters in active structural control. Journal of sound vibration, 173, 471-50.

Hallauer W. L., Skidmore G. R., and Mesquita L. C. (1982). Experimental – Theoretical study of active vibration control. "Proceedings of the International Modal Analysis Conference", Orlando, USA, pp. 39-45.

Liao C. Y., and Sung C. K. (1993). An elastodynamic analysis and control of flexible linkages using piezoceramic sensors and actuators. Journal of Mechanical Design, 115, 658-665.

Meirovitch L., and Baruh H. (1981). Optimal control of damped flexible gyroscopic systems. Journal of Guidance and Control, 4, 157-163.

Meirovitch L., and Baruh H. (1985). The implementation of modal filters for control of structures. Journal of Guidance and Control, 8(6), 707-716.

Preumont A. (2002). "Vibration Control of Active Structures: An Introduction" Kluwer Academic Publishers.

Singh S. P., Pruth H. S. i, and Agarwal V. P. (2003). Efficient modal control strategies for active control of vibrations. Journal of Sound and Vibration, 262, 563-575.

Song G., Schmidt S. P., and Agrawal B. N. (2000). Active vibration suppression of a flexible structure using smart material and modular control patch. Proc. Inst. Mech. Eng., 214, 217-229.

Sumali H., Meissner K., and Cudney H. H. (2001). A piezoelectric array for sensing vibration modal coordinates. Sensors and Actuators A, 93, 123-131.

Sun D., Mills J. K., Shan J., and Tso S. K. (2004). A PZT actuator control of a single-link flexible manipulator based on linear velocity feedback and actuator placement. Mechatronics, 14, 381–401.

Zhang X., Mills J. K., and Cleghorn W. L. (2009). Dynamic Modeling and Active Vibration Control of a Planar 3-PRR Parallel Manipulator with Three Flexible Links. PhD thesis, University of Toronto.

Zhang X., Mills J, K., and Cleghorn W. L. (2007). Dynamic Modeling and Experimental Validation of a 3-PRR Parallel Manipulator with Flexible Intermediate Link. Journal of Intelligent and Robotic Systems, 50 (4), 323-340